Published in final edited form as:
Neuropharmacology. 2012 June ; 62(7): 2429–2438. doi:10.1016/j.neuropharm.2012.02.017.

Chronic Intermittent Ethanol and Withdrawal Differentially Modulate Basolateral Amygdala AMPA-type Glutamate Receptor Function and Trafficking

Daniel T Christian[1], **Nancy J Alexander**[1], **Marvin R Diaz**[1,3], **Stacey Robinson**[2], and **Brian A McCool**[1,2]

[1]Department of Physiology and Pharmacology, Wake Forest School of Medicine, Winston-Salem, NC, USA

[2]Neuroscience and Alcohol Research Training Programs, Wake Forest School of Medicine, Winston-Salem, NC, USA

Abstract

The amygdala plays a critical role in the generation and expression of anxiety-like behaviors including those expressed following withdrawal (WD) from chronic intermittent ethanol (CIE) exposure. In particular, the BLA glutamatergic system controls the expression of both innate and pathological anxiety. Recent data suggests that CIE and WD may functionally alter this system in a manner that closely parallels memory-related phenomena like long term potentiation (LTP). We therefore specifically dissected CIE/WD-induced changes in glutamatergic signaling using electrophysiological and biochemical approaches with a particular focus on the plasticity-related components of this neurotransmitter system. Our results indicate that cortical glutamatergic inputs arriving at BLA principal via the external capsule undergo predominantly post-synaptic alterations in AMPA receptor function following CIE and WD. Biochemical analysis revealed treatment-dependent changes in AMPA receptor surface expression and subunit phosphorylation that are complemented by changes in total protein levels and/or phosphorylation status of several key, plasticity-associated protein kinases such as calcium/calmodulin-dependent protein kinase II (CaMKII) and protein kinase C (PKC). Together, these data show that CIE- and WD-induced changes in BLA glutamatergic function both functionally and biochemically mimic plasticity-related states. These mechanisms likely contribute to long-term increases in anxiety-like behavior following chronic ethanol exposure.

1. Introduction

For human alcoholics, withdrawal-associated anxiety is a major risk factor for relapse. The amygdala plays a critical role in the generation and expression of anxiety-like behaviors

Correspondence: Dr BA McCool, Department of Physiology and Pharmacology, Wake Forest Baptist Health School of Medicine, Medical Center Boulevard, Winston-Salem, NC 27157, USA. Tel: +1 336 716 8534; Fax: +1 336 716 8501; bmmcool@wakehealth.edu.
[3]Current Address: Dept. of Neurosciences, University of New Mexico Health Sciences Center, Albuquerque, NM, USA

DISCLOSURE
The authors declare no conflict of interest.

including those expressed following withdrawal from chronic ethanol exposure (Läck et al., 2005; Santucci et al., 2008). The lateral and basolateral subdivisions (BLA) form the primary input nuclei in the amygdala's emotion-related neural circuitry (Sah et al., 2003) and receive highly processed sensory information via cortical afferents coursing into the region from the external capsule (EC) (Rainnie et al., 1991). The BLA subsequently sends significant excitatory glutamate projections into areas like the central amygdala and the bed nucleus of the stria terminalis to drive the physiological and psychological manifestations of anxiety and fear (Davis et al., 1994). EC glutamatergic inputs are therefore a principal regulator of BLA principal neuron activity and help modulate the expression of anxiety-like behaviors included learned emotional responses. For example, experimental manipulation of BLA glutamatergic neurotransmission blocks innate anxiety responses as well as the acquisition/expression of learned fear in rodents (Rodrigues et al., 2001). We have recently demonstrated that inhibition of BLA glutamatergic neurotransmission can likewise down-regulate the expression of anxiety-like behaviors following withdrawal (WD) from chronic intermittent ethanol (CIE) exposure (Läck et al., 2007). Thus, the BLA glutamatergic system functions to regulate the expression of anxiety in both natural and pathological states.

Recent work has focused on glutamate neurotransmission in the BLA as a general target of modification by CIE exposure and WD. CIE/WD robustly increase both *N*-Methyl-D-aspartate receptor (NMDAR) and kainate receptor locally-evoked synaptic function in BLA pyramidal neurons (Floyd et al., 2003; Läck et al., 2008; Läck et al., 2009). However, both kainate receptor-dependent and NMDAR-dependent plasticity are occluded following both CIE and WD (Läck et al., 2009; Stephens et al., 2005). Specific functional changes of α-amino-3-hydroxy-5-methyl-4-isoxazolepropionic acid (AMPA) receptors (AMPAR) in response to CIE/WD have only been recently examined. In these studies, it was determined that the amplitude of AMPAR mediated miniature excitatory post synaptic currents (mEPSC) increased following WD (Läck et al., 2007). These functional studies suggest that CIE/WD up-regulate AMPAR function to induce plasticity-like state. This would suggest that chronic ethanol exposure engages the BLA glutamate system in a manner similar to experience-dependent long term potentiation (LTP). Given that the BLA receives numerous glutamatergic inputs and the anatomical origins of mEPSCs are not clear, it is uncertain whether the increased AMPAR function can be attributed to specific afferents or represents a more generalized feature of BLA glutamatergic synapses during/following chronic ethanol exposure.

There is a large body of literature describing the cellular and molecular mechanisms governing the generation and expression of LTP of glutamatergic synapses in the BLA (Blair et al., 2001; Maren, 2003; Sah et al., 2008). Postsynaptic forms of LTP can be initiated by several distinct mechanisms including NMDAR-dependent forms (Yu et al., 2008) as well as NMDAR-independent (Chapman and Bellavance, 1992) including those initiated by synaptic kainate receptors (Läck et al., 2008). Regardless of the initiation mechanism, the different forms of postsynaptic LTP are all characterized by increased AMPAR function and/or trafficking which are essential for the expression of postsynaptic LTP in the BLA (Makino and Malinow, 2009; Malenka, 2003; Malinow, 2003; Yu et al., 2008). In regions like the hippocampus, plasticity-associated increases in AMPAR function are strictly governed by the phosphorylation status of amino acid residues within specific AMPAR subunits (GluA1-4) (Boehm and Malinow, 2005; Wang et al., 2005). In this context, a multitude of protein kinases (Appleby et al., 2011; Boehm et al., 2006) appear to contribute to the regulation of AMPAR function and trafficking (Ahn and Choe, 2009; Boehm and Malinow, 2005). Given that CIE/WD alter glutamate receptor systems involved in LTP, we examined parallels between plasticity-related glutamatergic signaling components altered by CIE/WD. We specifically hypothesize that CIE/WD engage the BLA AMPAR system, including plasticity-associated kinases, similar to LTP.

2. Methods

2.1 Animals

Animals: Male Sprague-Dawley rats (Harlan, Indianapolis, IN, USA) weighing 100–150g (approximately 5–6 weeks of age) were group housed for the duration of the experiments. All experimental procedures were reviewed and approved by the WFUSM Animal Care and Use Committee and are consistent with the NIH Guidelines for the Care and Use of Laboratory Animals.

2.2 Chronic Intermittent Ethanol Exposure & Withdrawal

Chronic ethanol exposure was conducted in a manner similar to previous reports (Läck et al., 2009; Läck et al., 2007). Briefly, animals were placed into air-tight, Plexiglas enclosures in their home cages and exposed to either ethanol vapor (~37mg/L) or room air during the light cycle (12 hours/day) for 10 consecutive days. Animals receiving this chronic intermittent treatment were divided into two subgroups: 1) those euthanized while still intoxicated at the end of the last exposure (CIE) and 2) those euthanized 24 hours after the last exposure (WD). Control (CON) animals were housed in identical Plexiglas enclosures, exposed only to room air, and euthanized during the same weeks as the CIE and WD animals. Trunk blood was collected from the CIE group at euthanasia and analyzed for blood ethanol levels. At the time of brain extraction, blood ethanol levels in the CIE animals were 185.33 ± 5.75 mg/dL as determined by a commercially available alcohol dehydrogenase assay (Genzyme, Middleton WI, U.S.A.).

2.3 Electrophysiology methods

2.3.1 Slice Preparation—Electrophysiology experiments used coronal brain slices containing the amygdala from animals anesthetized using isoflurane (3%) and decapitated according to a Wake Forest Baptist Health institutional IACUC-approved protocol. Brains were removed and incubated in ice-cold sucrose-modified artificial cerebral spinal fluid (aCSF) equilibrated with 95% O_2 and 5% CO_2 containing (in mM): 180 sucrose, 30 NaCl, 4.5 KCl, 1 $MgCl_2 \cdot 6H_2O$, 26 $NaHCO_3$, 1.2 NaH_2PO_4, 100 ketamine, and 10 glucose. Brains were sliced (400μm) in the same solution on a Leica VT1200S Vibratome (Leica, Germany) or Vibratome Series 3000 (Vibratome, St. Louis, MO, U.S.A.) then submerged in room-temperature (~25°C), oxygenated standard aCSF containing (in mM): 126 NaCl, 3 KCl, 1.25 NaH_2PO_4, 2 $MgSO_4$, 26 $NaHCO_3$, 10 glucose, and 2 $CaCl_2 \cdot 2H_2O$. Slices were maintained in aCSF for ~1 hour before recording. Experiments were performed 1–5 hours after preparation of the BLA slices. All chemicals were obtained from Sigma-Aldrich (St. Louis, MO), Tocris (Ellisville, Missouri), or United States Pharmacopeia (Rockville, Maryland).

2.3.2 Whole-cell patch-clamp recording—Methods for whole-cell voltage clamp recordings from BLA neurons within slices were similar to those reported previously (Läck et al., 2007). Slices were placed in a recording chamber continuously perfused with room-temperature aCSF at a rate of 2.0 ml/min. Pipette resistances were 6–12 MΩ when electrodes were filled with an internal solution containing (in mM): 122 Cs-gluconate, 10 CsCl, 10 HEPES, 1 EGTA, 5 NaCl, 0.1 $CaCl_2$, 4 Mg-ATP, 0.3 Na-GTP, and 2 QX314-(Cl), pH 7.25, osmolarity 280–290 mOsm or 145 K-Gluconate, 5 NaCl, 1 $MgCl_2$, 10 EGTA, 10 HEPES, 2 Mg-ATP, 0.1 Na-GTP, pH 7.25, osmolarity 280–290. Data were acquired via Axopatch 700B or Axopatch 200B amplifiers (Axon Instruments, Foster City, CA) and stored for later analysis using pClamp software (Axon Instruments, Foster City, CA). Glutamatergic synaptic currents were pharmacologically isolated using GABAergic antagonists. Only neurons with a high membrane capacitance (>100pF) and low access resistance (<30MΩ) were considered presumptive principal neurons (Washburn and Moises, 1992) and included in the current analysis. Synaptic responses were evoked using constant-

voltage activation of concentric bipolar stimulating electrodes (FHC Inc., Bowdoin, ME) as previously described (Läck et al., 2009). Mean stimulation intensities across all experiments were 31 ± 3 mV and did not statistically vary across the different treatment groups ($P > 0.05$, $F(2,31) = 1.92$ One-way ANOVA).

2.3.3 Paired-pulse ratio—Paired-pulse ratios (PPR) were calculated with two equal-intensity electrical stimulations with a range of inter-pulse intervals (25–100 ms). A normalized ratio of the amplitudes of the evoked EPSCs was taken (second amplitude – first amplitude, divided by the first) to provide a conservative estimate of the second response amplitude (Schulz et al., 1995). All values are expressed as mean ± SEM.

2.3.4 Strontium Substitution—Experiments were conducted in aCSF where strontium (3.0mM) was substituted for calcium (2.0mM). This substitution allowed for the characterization of electrically evoked asynchronous EPSC (aEPSC) responses (Choi and Lovinger, 1997). A bipolar stimulator was placed in the external capsule and electrical square wave stimulation (0.4 ms) was applied every 30 seconds to elicit aEPSCs. Events were collected and stored for offline data analysis (Clampfit 10.2, Mini Analysis (Synaptosoft Fort Lee NJ). Semi-automated aEPSC analysis was conducted on responses starting 50 ms after the stimulation artifact to include responses during a 400 ms window (e.g. 50ms – 450ms post-stimulus) as previously described (Choi and Lovinger, 1997). Only this time interval was extracted for analysis using commercially-available software (MiniAnalysis, SynaptoSoft, Decatur, GA) to allow for the resolution of individual aEPSC events. Some recordings utilized bath application of insulin (1.0μM) as described in the text.

2.4 Western blots

Western blot procedures were similar to those in previously published reports (Diaz et al., 2011). Briefly, lysis buffer (10mM Tris pH 7.4, 2.0% sodium dodecyl sulfate, 1mM EDTA pH 8, protease inhibitors for mammalian tissue (Sigma, St. Louis, MO), and phosphatase inhibitor cocktail 1 &2 [Sigma]) was added to BLA samples dissected from CON, CIE, and WD coronal brain slices at 7μl/mg tissue, disrupted by brief sonication on ice, and incubated at 4°C on a rotisserie mixer for 1 hour. Protein yield was quantified using a BCA assay (Pierce Chemical, Rockford, IL).

Five to twenty micrograms of total protein was loaded on to 4–20% sodium dodecyl sulfate precast polyacrylamide gels (Pierce Chemical, Rockford, IL) or 8–16% GELS (Biorad), separated, and transferred to a nitrocellulose membrane (Hybond N; Amersham, Piscataway, NJ). Membranes were blocked with Tris buffered saline (TBS)-T (150mM NaCl, 5.2 mM Na_2HPO4, 1.7mM KH_2PO_4, 0.05% Tween-20) containing 5% bovine serum albumin (BSA) or 5% milk. Subsequently, blots were incubated overnight at 4°C or for 3hrs at 25°C in TBS-T/1.0% BSA containing target specific primary antibodies. The following antibodies exhibited specificity for the protein targets as indicated by immunoreactive bands at expected molecular weights: PKCγ (1:2000) and Neurogranin (1:2000) from Abcam (Cambridge, MA); GluA1 (1:3000), GluA1 phosphoSer845 (1:1000), GluA2/3 (1:4000), and GluA2 phosphoSer831 (1:1000) from Chemicon (now Millipore, Billerica, MA); PKCα (0.5μg/ml) from Millipore; CaMKIIα phosphosThr305/306 (1:1000) from PhosphoSolutions (Aurora, CO); CaMKIIα (1:20,000) and CaMKIIα phosphoThr286 (1:1000) from Thermo Scientific (Waltham, MA); GluA2 phosphoSer880 (1:1000) and Neurogranin phosphoSer36 (1:1000) from Upstate (now Millipore). Following extensive washing with TBS-T, the blots were exposed to HRP-labeled secondary antibodies for one hour at room temperature with agitation. Secondary antibodies were either Goat×Rabbit (1:3000) for the polyclonal antisera or Goat×Mouse (1:3000) for the monoclonal primary antibodies and were both from Sigma (St. Louis, MO). Detection of bound secondary antibody was performed using enhanced

chemiluminescence (Pierce) while band intensity was quantified from digital images using a Chemidoc and Quantity One Software (Biorad). Single blots contained protein samples from all three treatment groups (CON, CIE, and WD tissue) with each lane corresponding to total BLA protein from an individual animal. For analysis CON animal expression was averaged; and all samples were normalized against the CON mean within each gel with data being expressed as a percent CON unless otherwise noted. Experiments were performed in duplicate.

2.4.1 Cross-linking BS^3 treatment—To examine surface-expression of glutamatergic receptor subunits, we utilized a membrane-impermeable cross-linker bis(sulfosuccinimidyl)suberate (BS^3, Thermal Scientific) as previously described (Clayton et al., 2002). Surface expression was determined in slices from CON, CIE, and WD slices following 1 hour equilibration in aCSF or aCSF containing 1mg/ml BS^3 at 4°C followed by 5 minute rinses with rinsing solution (aCSF-20mM Tris, pH = 7.4) for 5 minutes. Rinses were repeated 3 times, and the BLA was then dissected and frozen until used for Western Blot analysis. Analysis compared BS^3-sensitive protein expressed as percent of total protein from the aCSF-treated control slices across the three exposure groups.

2.5 Data Analysis

All values are expressed as mean ± SEM. Primary statistical analyses were conducted using one-way ANOVAs with $p < 0.05$ considered statistically significant. Significant group differences were measured using Newman-Keuls post-hoc tests.

3. RESULTS

3.1 CIE/WD Alter Postsynaptic Function at the EC-BLA input

Utilizing a paired pulse protocol we examined presynaptic function at EC-BLA synapses in slices from CON, CIE, and WD animals. EC stimulation across a wide range of inter-stimulus intervals (25, 50, 100 ms) showed no alteration in the paired-pulse ratio (PPR; Fig. 1). Since PPRs at short intervals are thought to reflect presynaptic alterations in the release probability of neurotransmitters (Andreasen and Hablitz, 1994), these findings indicated that there were no presynaptic effects of CIE or WD at the EC-BLA input.

To confirm the lack of presynaptic functional alterations at the EC-BLA input, we utilized electrically evoked responses in an extracellular solution containing strontium (Sr^{2+} = 3.0 mM) substituted for calcium (2.0 mM). Since strontium poorly substitutes for calcium during excitation-secretion (Dodge et al., 1969), electrically-evoked ‘synchronous’ synaptic responses in strontium are followed by asynchronous events (aEPSC) that reflect release from single synapses. Across our treatment groups, we found no differences in the inter-event interval of the aEPSCs (Fig. 2; CON 19.46 ± 1.27ms, n = 10; CIE, 17.88 ± 0.94ms, n = 13; WD, 16.72 ± 0.98ms, n = 7; ($F(2, 27) = 1.332$, $p > 0.05$). These data confirmed no treatment specific alterations in presynaptic function measured using paired-pulses. Conversely, WD increased aEPSC amplitudes compared to both CON and CIE slices. (Fig. 2, CON 8.87 ± 0.33pA, n = 10; CIE, 9.65 ± 0.73pA, n = 13; WD 12.60 ± 1.00pA, n = 7; ($F(2, 27) = 6.124$, $p < 0.01$ One Way ANOVA with Newman-Keuls Post hoc test). When viewed in the absence of presynaptic alterations, the increase in aEPSC amplitude in WD slices can be characterized as a purely post-synaptic alteration in AMPAR function.

3.2 Changes in Surface Receptor Expression during CIE & WD

To define the molecular mechanisms controlling increased AMPAR function following WD, we characterized receptor subunit expression and localization from CON, CIE, and WD BLA slices. There were no differences in total GluA1 protein expression levels between any

treatment group (Fig. 3, CON, 100.00 ± 9.24%, n = 8; CIE, 92.80 ± 3.71%, n = 8; WD, 105.16 ± 5.49% n = 7; F (2, 20) = 0.44 One Way ANOVA, $p > 0.05$). As with GluA1, there were no treatment-dependent changes in total GluA2/3 protein levels (Fig. 3, CON, 100.00 ± 6.30%, n = 8; CIE, 100.07 ± 4.71%, n = 8; WD, 105.44 ± 6.14%, n = 8; One Way ANOVA $F(2,21) = 0.292$ $p > 0.05$).

We examined the surface localization of GluA1 and GluA2/3 AMPAR subunits using tissue treatment with the membrane-impermeant, protein crosslinking agent bis-sulfosuccinimidyl suberate (BS^3) followed by western blot analysis. These studies indicate a WD-induced increase in the relative amount of BS^3-accessible GluA1 subunit protein compared to CON and CIE groups (Fig. 3; CON, 66.7 ± 6.7% of total protein, n = 4; CIE, 78.8 ± 1.8%, n = 4; WD, 90.0 ± 1.4%, n = 4; One Way ANOVA, $p < 0.01$ Newman-Keuls Post hoc test). We next examined GluA2/3 surface localization as reflected by BS^3-accessibility and found an increase in both CIE and WD groups compared to CON (Fig. 3, CON, 63.5 ± 5.8% n = 4; CIE, 78.4 ± 3.8% n = 4; WD, 89.4 ± 2.7%, n = 4; One Way ANOVA $p < 0.01$, Newman-Keuls post hoc tests). As a control for the membrane-impermeant BS^3 treatment, we also examined the effects of BS^3 exposure on the intracellular protein, beta-actin. As expected, beta-actin levels were unaffected by BS^3 treatment (Fig. 3, $+BS^3$, 100.00 ± 17.9% n = 4; $-BS^3$, 111.00 ± 16.9% n = 4; unpaired T-test, $p > 0.05$). These data indicate that CIE and WD alter the trafficking of AMPAR subunits from BS^3-inaccessible, presumably intracellular pools to the cell surface. This provides a potential mechanism for the increased amplitudes of DNQX-sensitive unitary aEPSCs.

3.3 CIE/WD dynamically alter GluAR phosphorylation

We next examined the phosphorylation status of AMPAR subunits following our treatment conditions as changes in phosphorylation are implicated in altered receptor trafficking. For example, phosphorylation of GluA1 Ser831 by Calcium/Calmodulin protein Kinase II (CaMKII)/Protein Kinase C (PKC) increases receptor function and surface trafficking (Barria et al., 1997; Wang et al., 2005). Western blot analysis indicated both CIE and WD increased phosphorylation at S831 (Fig. 4; CON, 100.00 ± 7.97% n = 4; CIE, 138.27 ± 8.04% n = 4, WD, 152.14 ± 14.41% n = 4; F (2, 9) = 8.463, One Way ANOVA $p < 0.01$, Newman-Keuls Post Hoc test). In addition to Ser831, phosphorylation of GluA1 Ser845, a putative Protein Kinase A (PKA) site, increases surface expression of GluA1 containing receptors in the hippocampus (Oh et al., 2006). However, Ser845 phosphorylation remained unchanged in CIE or WD BLA slices (Fig. 4, CON, 100.00 ± 5.38%, n = 4; CIE, 96.35 ± 3.24%, n = 4; WD, 109.15 ± 7.29%, n = 4; $F(2,9) = 1.405$, $p > 0.05$, One Way ANOVA). As with GluA1, GluA2 Ser880 phosphorylation is PKC-dependent (Famous et al., 2008) and regulates the stabilization of membrane bound GluA2R subunits, presumably by removing GluA2-containing receptors from the rapidly recycling pool (Famous et al., 2008; States et al., 2008; Wang et al., 2005). Phosphorylation at GluA2 Ser880 significantly increased following WD only (Fig. 4, CON, 100.00 ± 13.97%, n = 4; CIE, 162.98 ± 31.72%, n = 4; WD, 241.98 ± 31.21%, n = 4; $F(2,9) = 6.977$, $p < 0.05$, One Way ANOVA, Newman-Keuls Post hoc tests).

3.4 CaMKII & PKC

CaMKII is one of the protein kinases believed to control the phosphorylation status of GluA1 Ser831 (Moriguchi et al., 2009). We examined total CaMKIIα protein levels and found no significant difference between the treatment groups (Fig. 5, CIE 104.85 ± 4.17% n = 16; WD 97.26 ± 2.84% n = 16; CON 100.00 ± 3.13% n = 16; $F(2,46) = 1.247$, $p > 0.05$, One Way ANOVA). However, Thr286-phosphorylated CaMKII significantly increased following CIE and returned to CON levels during WD (Fig. 5, CON 100.00 ± 12.27%, n = 7; CIE 211.19 ± 49.49%, n = 8; WD 78.62 ± 11.99%, n = 7; $F(2,19) = 4.905$, $p < 0.05$ One

Way ANOVA, Newman-Keuls post hoc tests). Thr286 phosphorylation activates the kinase and converts it into an "autonomous" kinase that no longer requires calcium/calmodulin. Among the other mechanisms controlling CaMKII activity, phosphorylation at Thr305/306 typically occurs only *following* Thr286 phosphorylation, is autoinhibitory, and blocks further activation of CaMKII by reducing its sensitivity to Ca^{2+}/Calmodulin (Patton et al., 1990). Phosphorylation of CaMKII Thr305/306 increased during WD compared to both CON and CIE treatments (Fig. 5, CON 100.00 ± 11.24%, n = 9; CIE 106.53 ± 9.85%, n = 8; WD 142.18 ± 13.81%, n = 7; $F(2,21) = 3.617$, $p < 0.05$ One Way ANOVA, Newman-Keuls post hoc tests). These data suggest that CIE increases CaMKII activity via Thr286 phosphorylation. Subsequently, Thr286 de-phosphorylation along with Thr305/306 phosphorylation would shift the kinase to an inactive state during withdrawal.

PKC phosphorylates both GluA1 (Ser831) and GluA2 (Ser880) (Crombag et al., 2008) subunits contributing to altered receptor trafficking. We therefore measured total protein expression levels of conventional (α, γ) PKC isoforms. For the γ isoform, both CIE and WD decreased levels of PKCγ protein (Fig. 6, CIE, 72.90 ± 4.43% n = 4; WD, 52.62 ± 4.90% n = 4; CON, 100.00 ± 12.80% n = 4; $F(2,9) = 8.156$, $p < 0.01$ One Way ANOVA, Neuman Keuhls post hocs). There was also a significant main-effect of treatment on the total levels of PKCα but post hoc analysis did not reveal any significant treatment-specific differences (Fig. 6, CIE, 95.05 ± 5.25% n = 4; WD, 64.06 ± 6.66%, n = 4; CON, 100.00 ± 13.57% n = 4; $F(2,9) = 4.443$ $p < 0.045$, One Way ANOVA).

The treatment-dependent decease in conventional PKC total protein levels appears to contradict the level of phosphorylation of GluA1 Ser831 and GluA2 Ser 880; the latter is a known PKC phosphorylation site. This suggests that PKC activity and protein expression may not be regulated in parallel. To test this, we examined the phosphorylation status of a well-characterized substrate of conventional PKC isoforms, neurogranin (Ng) Ser36, and found a significant increase in Ng phosphorylation following CIE that returned to control levels during WD (Fig. 6, CON, 100.00 ± 8.28% n = 8; CIE, 184.45 ± 33.57%, n = 9; WD, 108.81 ± 9.29%, n = 7; $F(2,21) = 4.336$, $p < 0.05$ One Way ANOVA Neuman Keuhls post hoc). There was no change in total Ng protein expression (Fig. 6, CON, 100.00 ± 8.83%, n = 8; CIE, 107.55 ± 9.65%, n = 9; WD, 109.21 ± 8.79%, n = 9, $F(2,23) = 0.277$, $p > 0.76$ One Way ANOVA). Thus by two separate indicators of PKC kinase activity, GluA2 Ser880 and Ng Ser36 phosphorylation, indicate that conventional PKC activity is increased during CIE despite treatment-dependent down-regulation of total PKC protein levels.

3.5 CIE/WD Up-regulation of AMPAR Function is Reversible

Our protein expression data demonstrates a WD–induced down regulation of plasticity-related mechanisms (CaMKII/PKC) and suggests that signaling mechanisms that engage these kinases would be less efficacious in reversing increased AMPAR function/surface expression. However, insulin and insulin receptors have been previously described in the brain (Hill et al., 1986); and activation of insulin receptors induces functional (Spicarova and Palecek, 2010) structural changes (Chiu et al., 2008) at glutamatergic synapses. Insulin application also induces LTD at glutamatergic synapses in hippocampal culture and slice preparations (Beattie et al., 2000; Huang et al., 2004a) via AMPAR internalization. AMPAR regulation by insulin could therefore be independent of WD-induced down regulated kinase systems. Insulin application significantly reduced the amplitude of aEPSC events in both CON (Baseline 8.382 ± 0.624, insulin 7.228 ± 0.634; Paired t-test; $t = 8.076$, $df = 5$, $p < 0.01$; data not shown) and WD (Baseline 11.13 ± 1.145, insulin 8.072 ± 0.712; Paired t-test, $t = 5.782$, $df = 5$, $p < 0.01$, t-test data; data not shown). Importantly, the magnitude of insulin modulation was significantly larger in WD neurons (Fig. 7, % Baseline, Con, −14.09 ± 1.863%; WD, −26.89 ± 2.103%; Unpaired t-test $t = 4.555$ $df = 10$ $p < 0.01$). This finding

suggests that insulin-mediated AMPAR down-regulation pathways are still intact and are likely independent from CaMKII/PKC–dependent signaling pathways.

Discussion

4.1 Post but not Pre synaptic alterations of AMPAR function at External Capsule-BLA inputs following WD

The current studies did not reveal any presynaptic alterations of glutamate neurotransmission at the EC-BLA synapses with either paired-pulses or unitary aEPSC responses following CIE and WD. These findings are consistent with previous data from our lab (Läck et al., 2009) and allow us to study input specific post-synaptic alterations without contamination by presynaptic mechanisms. Enhanced AMPA mediated aEPSC amplitudes indicate a postsynaptic increase in AMPAR expression/function specific to this BLA input following CIE and WD. This potentially provides mechanistic insight for previous data showing increased field EPSP responses following CIE and WD at the EC-BLA input (Läck et al., 2009) and suggest that down-regulating postsynaptic glutamate signaling may reverse WD-related anxiety-like behaviors.

To this end we sought to down-regulate WD-induced functional increases in AMPAR signaling. Given that WD down regulated CaMKII and conventional PKC systems that control use-dependent decreases in synaptic efficacy, we looked for a tool that could down regulate AMPARs without directly requiring CaMKII or PKC. Activation of insulin receptors induces LTD-like functional (Spicarova and Palecek, 2010) alterations at glutamatergic synapses that involves AMPAR internalization (Beattie et al., 2000; Huang et al., 2004a). In our WD treatment group, insulin decreased aEPSC amplitudes suggesting the capacity for plastic changes via this signaling mechanism remains intact in CIE/WD BLA.

4.2 Receptor trafficking

Our data show a differential but robust increase in BS^3-sensitive AMPAR subunits suggesting increased trafficking to the cell surface following both CIE (GluA2/3) and WD (GluA1 & GluA2/3). It is important to note that increased AMPAR surface expression following CIE did not reflect increased functional responses as measured by aEPSC amplitudes in this treatment group (see Fig. 2) and may represent a trafficking response to CIE treatment that is not evident at the synapse. GluA2 and GluA3 are expressed solely by BLA pyramidal neurons and not by GABAergic interneurons (McDonald, 1994; McDonald, 1996); so the biochemical data for these subunits would likely be specific for the neurons sampled by our recordings. GluA1 is expressed in both BLA pyramidal and GABAergic interneurons, the latter cells making up only 5–10% of the neurons in the BLA (McDonald, 1982). While we cannot rule out some differential regulation of GluA1 subunits in the different cells, it is unlikely that GABAergic GluA1 made any substantial contribution to the signals in our biochemical analysis.

Alterations in AMPAR trafficking/surface expression play a critical role in the generation of LTP (Malinow, 2003; Yu et al., 2008). In particular, receptors containing GluA1 (Makino and Malinow, 2009; Williams et al., 2007) and GluA2 (Famous et al., 2008; Liu and Zukin, 2007) are primary targets of trafficking processes. GluA1R trafficking is increased and necessary for NMDAR dependent LTP initiation in the amygdala (Yu et al., 2008). GluA1 receptors were also up-regulated following LTP initiation *in vivo* (Williams et al., 2007). Associative learning (Rumpel et al., 2005) and contextual learning (Mitsushima et al., 2011) both require GluA1 trafficking to the membrane surface. Similar patterns of trafficking are also evident for GluA2Rs. Recent studies have shown LTP induction increases surface expression of GluA2 specific subunits (Kakegawa et al., 2004), while synaptic scaling

increases trafficking of GluA2Rs (Gainey et al., 2009). GluA2 incorporation into membranes following GluA2-lacking insertions may serve as a mechanism for consolidating LTP activity (Plant et al., 2006). Another study demonstrated that during LTP initiation there was trafficking of AMPARs to peri-synaptic sites, followed by translocation to synaptic sites during the expression phase of LTP (Yang et al., 2008) (also see (Makino and Malinow, 2009; Tao-Cheng et al., 2011)). Our data showing a subsequent increase in aEPSC amplitudes in WD BLA neurons is then likely due to consolidation of newly trafficked receptors within synaptic specializations. Overall, our data showing increased trafficking of AMPARs following CIE and WD parallel receptor trafficking data following LTP. It is likely that CIE and WD are engaging similar trafficking mechanisms to those shown during LTP experiments.

Receptor surface expression and trafficking are regulated by the phosphorylation state of specific AMPAR subunits [Ser831 (GluA1) and Ser 880 (GluA2)] both *in vivo* and *in vitro* (Elgersma et al., 2002; Famous et al., 2008; Malinow, 2003), Our CIE and WD treatment animals demonstrated increased AMPAR phosphorylation of GluA1 and GluA2/3 subunits at CaMKII/PKC sites, but not GluA1 PKA phosphorylation sites (Oh et al., 2006) that parallel those described in LTP experiments. GluA1 Ser831 phosphorylation is associated with LTP in a wide range of models (Moriguchi et al., 2009). Fewer studies have examined the phosphorylation of Ser880 on GluA2Rs following LTP and there have been a variety of functions assigned to phosphorylation of this site. Increased Ser880 phosphorylation decreases receptor surface expression (Matsuda et al., 1999). However, States and colleagues (States et al., 2008) reported that AMPARs remaining in the postsynaptic membrane were not subject to trafficking following Ser880 phosphorylation. In addition the authors postulate that GluA2 receptors phosphorylated at Ser880 are removed from the readily-trafficked pool of receptors and preferentially retained in synaptic sites compared to non-phosphorylated receptors. Our data on the phosphorylation status and functional up-regulation of AMPARs during CIE/WD are consistent with this interpretation.

4.3 CaMKII

We examined the protein expression levels of CaMKIIα, which is specifically expressed in BLA pyramidal neurons (McDonald et al., 2002), as a potential mechanism regulating the phosphorylation status of GluA subunits. The phosphorylation of CaMKII at Thr286 activates the kinase and serves to increase “autonomous” kinase activity (Davies et al., 2007); and, we found that CIE enhanced CaMKII Thr286 phosphorylation. This suggests a role for CaMKII in GluA1 Ser831 phosphorylation within this treatment group. Interestingly, the increased phosphorylation of CaMKII (Thr286) following CIE treatment returned to CON levels during WD despite persistent GluA1 Ser831 phosphorylation during withdrawal. Based on CaMKII’s role in LTP induction (Huang et al., 2004b; Lengyel et al., 2004; Yang et al., 2004) and the occlusion of calcium-dependent forms of LTP during both chronic ethanol and withdrawal (Läck et al., 2009), we expected CaMKII Thr286 phosphorylation would be increased in both CIE and WD groups. Regardless, CaMKII Thr286 phosphorylation is linked with increased GluA1R surface trafficking (Appleby et al., 2011). And, genetic point mutations of CaMKII (Thr286) that block phosphorylation attenuate LTP induction indicating CaMKII (Thr286) phosphorylation is required for activity-dependent plasticity (Giese et al., 1998). Our data indicate that chronic ethanol increases CaMKII activity and that this likely contributes to increased GluA1R phosphorylation/trafficking.

Following phosphorylation of Thr286, CaMKIIα can autophosphorylate Thr305/306; and, this inhibitory feed-back blocks further activation of CaMKII (Colbran, 1993; Patton et al., 1990). Thr305/306 phosphorylation attenuates plasticity-related synaptic changes in a wide range of experimental models and serves to regulate the set-point for metaplasticity (Zhang

et al., 2005) driven by autonomously active CaMKII (Pi et al., 2010). In the hippocampus for example, mimicking Thr305/306 phosphorylation blocked both LTP and learning (Elgersma et al., 2002). Other studies suggest Thr305/306 phosphorylation may regulate 'plasticity threshold' by limiting kinase activity (Davies et al., 2007). Since CaMKII-dependent signaling cascades also mediate long-term depression (Elgersma et al., 2002), increased Thr305/306 phosphorylation may underlie plasticity 'deficits' following chronic ethanol/WD and provide one potential cellular mechanisms that underlies the persistence of withdrawal-like states in rodent models and human alcoholics.

4.4 PKC

Multiple PKC isoforms are involved in the regulation of glutamate receptor function (Yang et al., 2004). For example, PKC-dependent phosphorylation of GluA2 Ser880 during LTP increases trafficking of AMPAR to the cell surface (Famous et al., 2008) and stabilizes membrane bound receptors by removing them from readily-trafficked pools (States et al., 2008). Given the persistent phosphorylation of GluA2 Ser880 in our results, we hypothesized that CIE and WD would up-regulate PKC protein expression or activity. We found instead that total protein levels of PKCα and γ isoforms were decreased following CIE and especially WD. Since our analysis focuses only on a limited number of time points, increases in total PKC protein levels could occur earlier or more transiently. Alternatively, total protein levels do not necessarily correspond with kinase activity. We found that neurogranin, a substrate of PKC, is reversibly phosphorylated during CIE. This indirect measure suggests elevated PKC activity during the chronic ethanol exposure could contributed to GluA3 Ser880 phosphorylation. Ethanol has also been shown to modulate PKC intracellular localization (Wilkie et al., 2007); and we cannot rule out contributions by and alterations within this PKC-signaling mechanism as well. Finally, it is noteworthy that nothing is known about the cellular localization of PKC isoforms or Ng in the various BLA cell types. While we cannot rule out some contribution by PKC or Ng localized to GABAergic interneurons, this heterogeneous population of cells represents a relatively modest number of neurons (5–10%) compared to the pyramidal projection neurons (McDonald, 1982). Similar to the effects of WD on CaMKII, a down regulated conventional PKC system would be less effective in generating plasticity and support a persistent withdrawal-like state.

4.4.1 Interactions between PKC and CaMKII—In addition to being a target of PKC activity, neurogranin (Ng) functionally regulates calmodulin (CaM) availability to intracellular signaling pathways (Díez-Guerra, 2010; Huang et al., 2004b; Zhong et al., 2009). Non-phosphorylated Ng binds CaM and prevents it from interacting with calcium (Zhabotinsky et al., 2006). Elevated calcium levels initiate the release of CaM from Ng allowing CaM to bind to calcium and interact with CaMKII (Díez-Guerra, 2010; Zhong et al., 2009). PKC-dependent phosphorylation of Ng reduces CaM binding affinity, increasing the time CaM can interact with calcium and other signaling partners like CaMKII. Increased Ng phosphorylation indicates that CaM would be more persistently available to activate CaMKII. It is certainly feasible that this could facilitate CaMKII (Thr286) phosphorylation and induction of an LTP-like state. These data provide some of the first evidence for dynamic regulation of Ng by chronic drug treatment.

5. Summary

Our data demonstrate remarkable parallels between stereotypical postsynaptic LTP induction and expression in the amygdala and those induced by chronic ethanol exposure. In particular, CIE exposure appears to 'prime' the glutamate system by enhancing intracellular signaling pathways and moving AMPAR to the cell surface; while WD appears to convert

the glutamate system to a more persistent LTP-like state at the synapse. Multiple intracellular signaling pathways involved in expression, surface trafficking, and phosphorylation of receptors/kinases are also impacted by our treatments. These data suggest possible biochemical mechanisms that underlie the chronic ethanol-dependent occlusion of LTP induction/expression in the literature. It is particularly noteworthy that multiple signaling systems critical for plasticity-like alterations, many of which are necessary for down-regulation of the glutamate neurotransmitter system, are taken off-line or down-regulated during withdrawal. If specific phosphorylation states or kinase-dependent alterations can be reversed it may be possible to re-engage plasticity related mechanisms to create a new homeostatic set point that differs from the addiction/withdrawal set point. Our insulin data serves as an excellent example. This type of reversal may be crucial for increasing positive outcomes for alcohol dependence.

Acknowledgments

This work was funded by National Institutes of Health grants R01 AA014445 (BAM) and institutional training grants T32 AA007565 (BAM/SR) and T32 NS007422 (R. Oppenheim/SR).

References

Ahn SM, Choe ES. Alterations in GluR2 AMPA receptor phosphorylation at serine 880 following group I metabotropic glutamate receptor stimulation in the rat dorsal striatum. J Neurosci Res. 2009; 88:992–999. [PubMed: 19908285]

Andreasen M, Hablitz JJ. Paired-pulse facilitation in the dentate gyrus: a patch-clamp study in rat hippocampus in vitro. J Neurophysiol. 1994; 72:326–336. [PubMed: 7965017]

Appleby VJ, Corrêa SAL, Duckworth JK, Nash JE, Noël J, Fitzjohn SM, Collingridge GL, Molnár E. LTP in hippocampal neurons is associated with a CaMKII-mediated increase in GluA1 surface expression. J Neurochem. 2011; 116:530–543. [PubMed: 21143596]

Barria A, Muller D, Derkach V, Griffith LC, Soderling TR. Regulatory phosphorylation of AMPA-type glutamate receptors by CaM-KII during long-term potentiation. Science. 1997; 276:2042–2045. [PubMed: 9197267]

Beattie EC, Carroll RC, Yu X, Morishita W, Yasuda H, von Zastrow M, Malenka RC. Regulation of AMPA receptor endocytosis by a signaling mechanism shared with LTD. Nat Neurosci. 2000; 3:1291–1300. [PubMed: 11100150]

Blair HT, Schafe GE, Bauer EP, Rodrigues SM, LeDoux JE. Synaptic plasticity in the lateral amygdala: a cellular hypothesis of fear conditioning. Learn Mem. 2001; 8:229–242. [PubMed: 11584069]

Boehm J, Kang MG, Johnson RC, Esteban J, Huganir RL, Malinow R. Synaptic incorporation of AMPA receptors during LTP is controlled by a PKC phosphorylation site on GluR1. Neuron. 2006; 51:213–225. [PubMed: 16846856]

Boehm J, Malinow R. AMPA receptor phosphorylation during synaptic plasticity. Biochem Soc Trans. 2005; 33:1354–1356. [PubMed: 16246117]

Chapman PF, Bellavance LL. Induction of long-term potentiation in the basolateral amygdala does not depend on NMDA receptor activation. Synapse. 1992; 11:310–318. [PubMed: 1354397]

Chiu SL, Chen CM, Cline HT. Insulin receptor signaling regulates synapse number, dendritic plasticity, and circuit function *in vivo*. Neuron. 2008; 58:708–719. [PubMed: 18549783]

Choi S, Lovinger DM. Decreased frequency but not amplitude of quantal synaptic responses associated with expression of corticostriatal long-term depression. J Neurosci. 1997; 17:8613–8620. [PubMed: 9334432]

Clayton DA, Grosshans DR, Browning MD. Aging and surface expression of hippocampal NMDA receptors. J Biol Chem. 2002; 277:14367–14369. [PubMed: 11891215]

Colbran RJ. Inactivation of Ca^{2+}/calmodulin-dependent protein kinase II by basal autophosphorylation. J Biol Chem. 1993; 268:7163–7170. [PubMed: 8385100]

Crombag HS, Sutton JM, Takamiya K, Lee HK, Holland PC, Gallagher M, Huganir RL. A necessary role for GluR1 serine 831 phosphorylation in appetitive incentive learning. Behavioural Brain Res. 2008; 191:178–183.

Davies KD, Alvestad RM, Coultrap SJ, Browning MD. αCaMKII autophosphorylation levels differ depending on subcellular localization. Brain Res. 2007; 1158:39–49. [PubMed: 17559813]

Davis M, Rainnie D, Cassell M. Neurotransmission in the rat amygdala related to fear and anxiety. Trends Neurosci. 1994; 17:208–214. [PubMed: 7520203]

Diaz MR, Christian DT, Anderson NJ, McCool BA. Chronic ethanol and withdrawal differentially modulate lateral/basolateral amygdala paracapsular and local GABAergic synapses. J Pharmacol Exper Therap. 2011; 337:162–170. [PubMed: 21209156]

Díez-Guerra FJ. Neurogranin, a link between calcium/calmodulin and protein kinase C signaling in synaptic plasticity. IUBMB Life. 2010; 62:597–606. [PubMed: 20665622]

Dodge FA Jr, Miledi R, Rahamimoff R. Strontium and quantal release of transmitter at the neuromuscular junction. J Physiol. 1969; 200:267–283. [PubMed: 4387376]

Elgersma Y, Fedorov NB, Ikonen S, Choi ES, Elgersma M, Carvalho OM, Giese KP, Silva AJ. Inhibitory autophosphorylation of CaMKII controls PSD association, plasticity, and learning. Neuron. 2002; 36:493–505. [PubMed: 12408851]

Famous KR, Kumaresan V, Sadri-Vakili G, Schmidt HD, Mierke DF, Cha JHJ, Pierce RC. Phosphorylation-dependent trafficking of GluR2-containing AMPA receptors in the nucleus accumbens plays a critical role in the reinstatement of cocaine seeking. J Neurosci. 2008; 28:11061–11070. [PubMed: 18945913]

Floyd DW, Jung KY, McCool BA. Chronic ethanol ingestion facilitates N-methyl-D-aspartate receptor function and expression in rat lateral/basolateral amygdala neurons. J Pharmacol Exp Ther. 2003; 307:1020–1029. [PubMed: 14534353]

Gainey MA, Hurvitz-Wolff JR, Lambo ME, Turrigiano GG. Synaptic scaling requires the GluR2 subunit of the AMPA receptor. J Neurosci. 2009; 29:6479–6489. [PubMed: 19458219]

Giese KP, Fedorov NB, Filipkowski RK, Silva AJ. Autophosphorylation at Thr286 of the α calcium-calmodulin kinase II in LTP and learning. Science. 1998; 279:870–873. [PubMed: 9452388]

Hill JM, Lesniak MA, Pert CB, Roth J. Autoradiographic localization of insulin receptors in rat brain: Prominence in olfactory and limbic areas. Neuroscience. 1986; 17:1127–1138. [PubMed: 3520377]

Huang CC, Lee CC, Hsu KS. An investigation into signal transduction mechanisms involved in insulin-induced long-term depression in the CA1 region of the hippocampus. J Neurochem. 2004a; 89:217–231. [PubMed: 15030406]

Huang KP, Huang FL, Jager T, Li J, Reymann KG, Balschun D. Neurogranin/RC3 enhances long-term potentiation and learning by promoting calcium-mediated signaling. J Neurosci. 2004b; 24:10660–10669. [PubMed: 15564582]

Kakegawa W, Tsuzuki K, Yoshida Y, Kameyama K, Ozawa S. Input- and subunit-specific AMPA receptor trafficking underlying long-term potentiation at hippocampal CA3 synapses. Eur J Neurosci. 2004; 20:101–110. [PubMed: 15245483]

Läck AK, Ariwodola OJ, Chappell AM, Weiner JL, McCool BA. Ethanol inhibition of kainate receptor-mediated excitatory neurotransmission in the rat basolateral nucleus of the amygdala. Neuropharmacol. 2008; 55:661–668.

Läck AK, Christian DT, Diaz MR, McCool BA. Chronic ethanol and withdrawal effects on kainate receptor-mediated excitatory neurotransmission in the rat basolateral amygdala. Alcohol. 2009; 43:25–33. [PubMed: 19185207]

Läck AK, Diaz MR, Chappell A, DuBois DW, McCool BA. Chronic ethanol and withdrawal differentially modulate pre- and postsynaptic function at glutamatergic synapses in rat basolateral amygdala. J Neurophysiol. 2007; 98:3185–3196. [PubMed: 17898152]

Läck AK, Floyd DW, McCool BA. Chronic ethanol ingestion modulates proanxiety factors expressed in rat central amygdala. Alcohol. 2005; 36:83–90. [PubMed: 16396741]

Lengyel I, Voss K, Cammarota M, Bradshaw K, Brent V, Murphy KPSJ, Giese KP, Rostas JAP, Bliss TVP. Autonomous activity of CaMKII is only transiently increased following the induction of

long-term potentiation in the rat hippocampus. European J Neurosci. 2004; 20:3063–3072. [PubMed: 15579161]

Liu SJ, Zukin RS. Ca^{2+}-permeable AMPA receptors in synaptic plasticity and neuronal death. Trends Neurosci. 2007; 30:126–134. [PubMed: 17275103]

Makino H, Malinow R. AMPA receptor incorporation into synapses during LTP: the role of lateral movement and exocytosis. Neuron. 2009; 64:381–390. [PubMed: 19914186]

Malenka RC. Synaptic plasticity and AMPA receptor trafficking. Ann N Y Acad Sci. 2003; 1003:1–11. [PubMed: 14684431]

Malinow R. AMPA receptor trafficking and long-term potentiation. Philos Trans R Soc Lond B Biol Sci. 2003; 358:707–714. [PubMed: 12740116]

Maren S. The amygdala, synaptic plasticity, and fear memory. Ann N Y Acad Sci. 2003; 985:106–113. [PubMed: 12724152]

Matsuda S, Mikawa S, Hirai H. Phosphorylation of serine-880 in GluR2 by protein kinase C prevents its C terminus from binding with glutamate receptor-interacting protein. J Neurochem. 1999; 73:1765–1768. [PubMed: 10501226]

McDonald AJ. Neurons of the lateral and basolateral amygdaloid nuclei: A golgi study in the rat. J Comp Neurol. 1982; 212:293–312. [PubMed: 6185547]

McDonald AJ. Neuronal localization of glutamate receptor subunits in the basolateral amygdala. Neuroreport. 1994; 6:13–16. [PubMed: 7535573]

McDonald AJ. Localization of AMPA glutamate receptor subunits in subpopulations of non-pyramidal neurons in the rat basolateral amygdala. Neurosci Lett. 1996; 208:175–178. [PubMed: 8733298]

McDonald AJ, Muller JF, Mascagni F. GABAergic innervation of alpha type II calcium/calmodulin-dependent protein kinase immunoreactive pyramidal neurons in the rat basolateral amygdala. J Comp Neurol. 2002; 446:199–218. [PubMed: 11932937]

Mitsushima D, Ishihara K, Sano A, Kessels HW, Takahashi T. Contextual learning requires synaptic AMPA receptor delivery in the hippocampus. Proc Natl Acad Sci. 2011; 108:12503–12508. [PubMed: 21746893]

Moriguchi S, Han F, Shioda N, Yamamoto Y, Nakajima T, Nakagawasai O, Tadano T, Yeh JZ, Narahashi T, Fukunaga K. Nefiracetam activation of CaM kinase II and protein kinase C mediated by NMDA and metabotropic glutamate receptors in olfactory bulbectomized mice. J Neurochem. 2009; 110:170–181. [PubMed: 19457128]

Oh MC, Derkach VA, Guire ES, Soderling TR. Extrasynaptic membrane trafficking regulated by GluR1 serine 845 phosphorylation primes AMPA receptors for long-term potentiation. J Biol Chem. 2006; 281:752–758. [PubMed: 16272153]

Patton BL, Miller SG, Kennedy MB. Activation of type II calcium/calmodulin-dependent protein kinase by Ca2+/calmodulin is inhibited by autophosphorylation of threonine within the calmodulin-binding domain. J Biol Chem. 1990; 265:11204–11212. [PubMed: 2162838]

Pi HJ, Otmakhov N, Lemelin D, De Koninck P, Lisman J. Autonomous CaMKII can promote either long-term potentiation or long-term depression, depending on the state of T305/T306 phosphorylation. J Neurosci. 2010; 30:8704–8709. [PubMed: 20592192]

Plant K, Pelkey KA, Bortolotto ZA, Morita D, Terashima A, McBain CJ, Collingridge GL, Isaac JTR. Transient incorporation of native GluR2-lacking AMPA receptors during hippocampal long-term potentiation. Nat Neurosci. 2006; 9:602–604. [PubMed: 16582904]

Rainnie DG, Asprodini EK, Shinnick-Gallagher P. Excitatory transmission in the basolateral amygdala. J Neurophysiol. 1991; 66:986–998. [PubMed: 1684383]

Rodrigues SM, Schafe GE, LeDoux JE. Intra-amygdala blockade of the NR2B subunit of the NMDA receptor disrupts the acquisition but not the expression of fear conditioning. J Neurosci. 2001; 21:6889–6896. [PubMed: 11517276]

Rumpel S, LeDoux J, Zador A, Malinow R. Postsynaptic receptor trafficking underlying a form of associative learning. Science. 2005; 308:83–88. [PubMed: 15746389]

Sah P, Faber ES, Lopez De Armentia M, Power J. The amygdaloid complex: anatomy and physiology. Physiol Rev. 2003; 83:803–834. [PubMed: 12843409]

Sah P, Westbrook RF, Lüthi A. Fear Conditioning and Long-term Potentiation in the Amygdala. Annals N Y Acad Sci. 2008; 1129:88–95.

Santucci AC, Cortes C, Bettica A, Cortes F. Chronic ethanol consumption in rats produces residual increases in anxiety 4 months after withdrawal. Behav Brain Res. 2008; 188:24–31. [PubMed: 18061285]

Schulz PE, Cook EP, Johnston D. Using paired-pulse facilitation to probe the mechanisms for long-term potentiation (LTP). J Physiol Paris. 1995; 89:3–9. [PubMed: 7581296]

Spicarova D, Palecek J. Modulation of AMPA excitatory postsynaptic currents in the spinal cord dorsal horn neurons by insulin. Neuroscience. 2010; 166:305–311. [PubMed: 20005924]

States BA, Khatri L, Ziff EB. Stable synaptic retention of serine-880-phosphorylated GluR2 in hippocampal neurons. Molec Cell Neurosci. 2008; 38:189–202. [PubMed: 18417360]

Stephens DN, Ripley TL, Borlikova G, Schubert M, Albrecht D, Hogarth L, Duka T. Repeated ethanol exposure and withdrawal impairs human fear conditioning and depresses long-term potentiation in rat amygdala and hippocampus. Biol Psychiatry. 2005; 58:392–400. [PubMed: 16018978]

Tao-Cheng JH, Crocker VT, Winters CA, Azzam R, Chludzinski J, Reese TS. Trafficking of AMPA receptors at plasma membranes of hippocampal neurons. J Neurosci. 2011; 31:4834–4843. [PubMed: 21451021]

Wang JQ, Arora A, Yang L, Parelkar NK, Zhang G, Liu X, Choe ES, Mao L. Phosphorylation of AMPA receptors: mechanisms and synaptic plasticity. Mol Neurobiol. 2005; 32:237–249. [PubMed: 16385140]

Washburn MS, Moises HC. Electrophysiological and morphological properties of rat basolateral amygdaloid neurons in vitro. J Neurosci. 1992; 12:4066–4079. [PubMed: 1403101]

Wilkie MB, Besheer J, Kelley SP, Kumar S, O'Buckley TK, Morrow AL, Hodge CW. Acute ethanol administration rapidly increases phosphorylation of conventional protein kinase C in specific mammalian brain regions *in vivo*. Alcohol Clin Exper Res. 2007; 31:1259–1267. [PubMed: 17511744]

Williams JM, Guévremont D, Mason-Parker SE, Luxmanan C, Tate WP, Abraham WC. Differential trafficking of AMPA and NMDA receptors during long-term potentiation in awake adult animals. J Neurosci. 2007; 27:14171–14178. [PubMed: 18094256]

Yang HW, Hu XD, Zhang HM, Xin WJ, Li MT, Zhang T, Zhou LJ, Liu XG. Roles of CaMKII, PKA, and PKC in the induction and maintenance of LTP of C-fiber-evoked field potentials in rat spinal dorsal horn. J Neurophysiol. 2004; 91:1122–1133. [PubMed: 14586032]

Yang Y, Wang X-b, Frerking M, Zhou Q. Delivery of AMPA receptors to perisynaptic sites precedes the full expression of long-term potentiation. Proc Natl Acad Sci. 2008; 105:11388–11393. [PubMed: 18682558]

Yu SY, Wu DC, Liu L, Ge Y, Wang YT. Role of AMPA receptor trafficking in NMDA receptor-dependent synaptic plasticity in the rat lateral amygdala. J Neurochem. 2008; 106:889–899. [PubMed: 18466342]

Zhabotinsky AM, Camp RN, Epstein IR, Lisman JE. Role of the neurogranin concentrated in spines in the induction of long-term potentiation. J Neurosci. 2006; 26:7337–7347. [PubMed: 16837580]

Zhang L, Kirschstein T, Sommersberg B, Merkens M, Manahan-Vaughan D, Elgersma Y, Beck H. Hippocampal synaptic metaplasticity requires inhibitory autophosphorylation of Ca^{2+}/calmodulin-dependent kinase II. J Neurosci. 2005; 25:7697–7707. [PubMed: 16107656]

Zhong L, Cherry T, Bies CE, Florence MA, Gerges NZ. Neurogranin enhances synaptic strength through its interaction with calmodulin. EMBO J. 2009; 28:3027–3039. [PubMed: 19713936]

Highlights

- CIE/WD dynamically regulate postsynaptic AMPA receptor function and trafficking.
- Subunit specific alterations of AMPAR trafficking are phosphorylation dependent.
- Treatment specific alterations of protein kinase may regulate dynamic AMPAR phosphorylation.
- CIE/WD induce plastic like changes that mimic those demonstrated following LTP

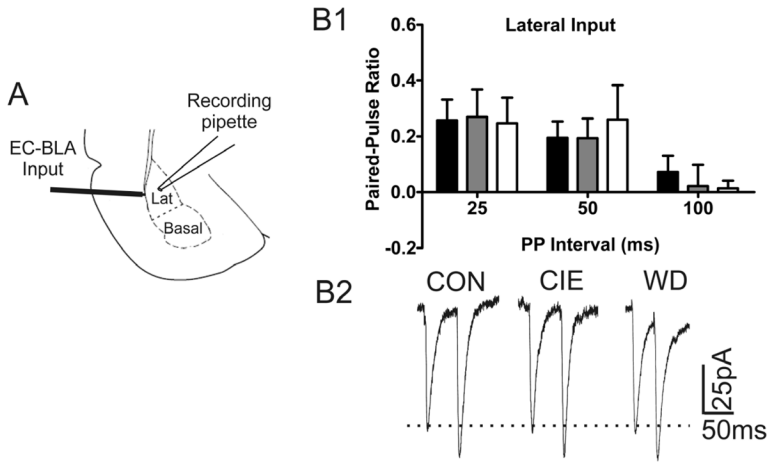

Figure 1. Lack of Treatment effect on Paired Pulse Ratios

A) Diagram indicating approximate stimulating electrode and recoding pipette placement in the External Capsule input into the BLA. B) No treatment dependent alterations of paired pulse ratios using evoked EPSCs across a range of inter-stimulus intervals. 25ms; CON [0.2574 ± 0.073, n = 11], CIE [0.2699 ± 0.098, n = 13]; WD [0.2468 ± 0.091 n = 5]; $F(2,26) = 0.0124$, $p > 0.05$; 50ms, CON [0.1953 ± 0.057, n = 11]; CIE [0.1938 ± 0.069, n = 13]; WD [0.2601 ± 0.123 n = 6], $F(2,27) = 0.1758$, $p > 0.05$; 100ms, CON [0.0726 ± 0.057, n = 10]; CIE [0.0224 ± 0.075, n = 13]; WD [0.0141 ± 0.026 n = 7]; $F(2,27) = .2123$ $p > 0.05$. B2) Representative traces of PPR during 50ms inter-event interval showing no alteration in PPR across treatment groups.

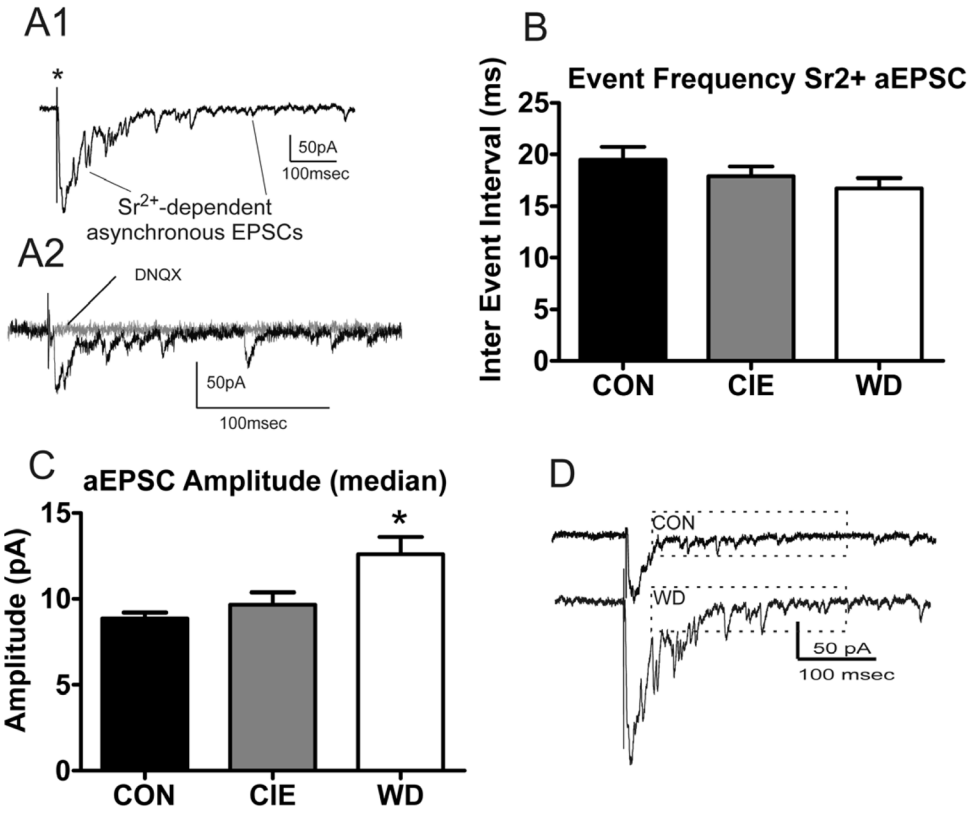

Figure 2. Post but not presynaptic alterations following WD as measured by Sr^{2+} substituted aEPSCs

A1 & A2) A1, Representative traces showing stimulated asynchronous release following Sr2+ substitution (3.0mM) for calcium (2.0mM) that are DNQX sensitive(A2). B) aEPSC event frequency at EC-BLA synapses does not change across treatment conditions (CON, n = 10; CIE n = 13; WD, n = 7). C) aEPSC amplitudes increased during WD compared to CON and CIE conditions (CON, n = 10; CIE, n = 13; WD, n = 7; * = $p < 0.01$ D) Representative traces showing increased amplitudes during WD compared to control. Dashed lines indicate area included in the analysis.

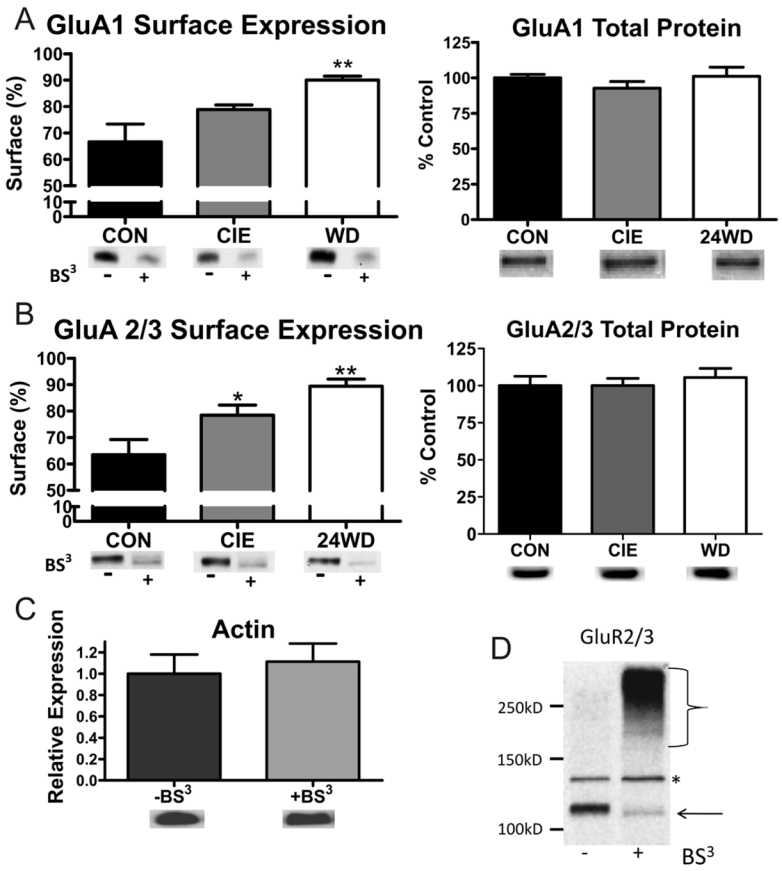

Figure 3. Treatment dependent increases in AMPAR surface expression

A) WD significantly increases BS3 sensitive surface accessible GluA1 containing AMPAR (n = 4 in all conditions, ** = $p < 0.01$; 20 μg/lane), with no change in GluA1total protein expression (CON n = 8; CIE n = 8; WD, n = 7; ~110 kD, 10 μg/lane). B) CIE significantly increases BS^3 sensitive surface accessible GluA2/3 containing AMPAR surface expression with a further increase in surface accessible receptors during WD (n = 4 in all conditions; * = $p > 0.05$, ** = $p < 0.01$; 20 μg protein/lane), with no change in GluA2/3 total protein expression (n = 8 in all conditions; ~108 kD, 10 μg protein/lane). C) No differences in expression of Beta actin (~43 kD) following BS^3 treatment (n = 4 in both conditions). D) Representative blots demonstrating BS^3 treatment decreasing mobility of BS^3 sensitive GluA2/3 AMPAR. *, denotes non-specific band. ←, Denotes location of intracellular portion of GluA2/3 protein.

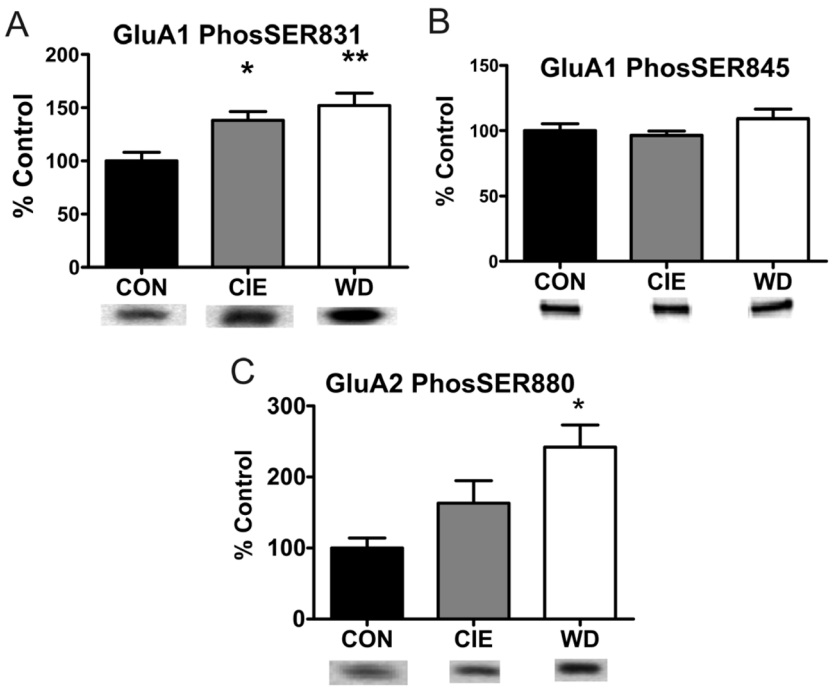

Figure 4. Site specific increases in AMPAR phosphorylation following CIE and WD exposure

A) Increased phosphorylation at Ser831 on GluA1Rs following CIE and WD (n = 4 in all conditions, * = $p < 0.05$, ** = $p < 0.01$; ~110 kD, 20 μg protein/lane) with no change in total protein levels (see Fig. 3). Ser831 is a known CaMKII and PKC phosphorylation site. Increased phosphorylation at this site increases receptor trafficking to the membrane surface. B) No change in PKA dependent phosphorylation of Ser845 on GluA1 containing receptors (n = 4 in all conditions; ~110 kD; 20 μg protein/lane). Demonstrates site specific increases in phosphorylation are not due to global increases in phosphorylation state. C) Increased phosphorylation of Ser880 on GluA2 containing receptors following WD (n = 4 in all conditions, * = $p < 0.05$; ~108 kD, 20 μg protein/lane) with no change in total protein (see Fig.3). Ser880 phosphorylation can be PKC dependent with increased phosphorylation serving to increase surface trafficking and/or reduce receptor internalization.

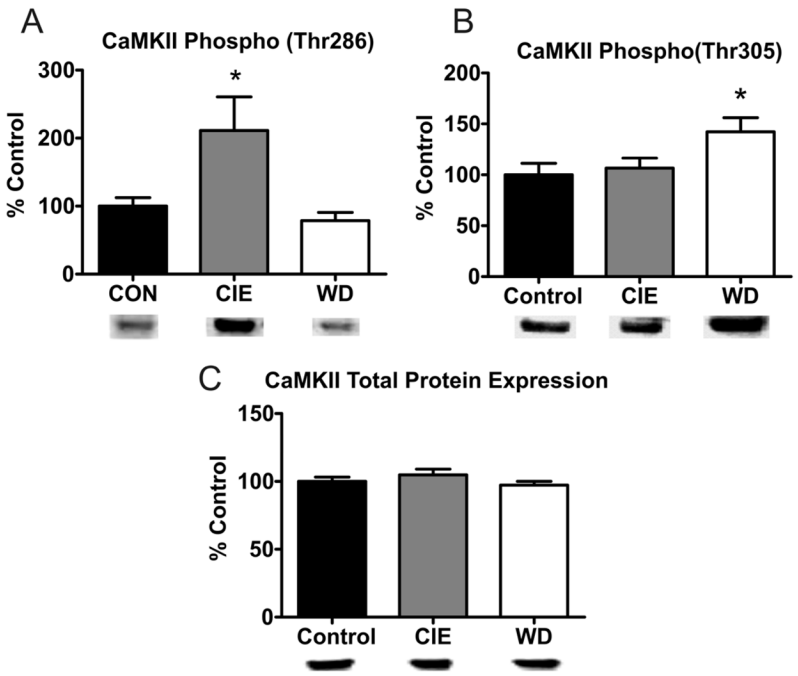

Figure 5. Dynamic Increases in CaMKII phosphorylation across CIE and WD

A) Increased Thr286 phosphorylation during CIE compared to both CON and WD conditions (CON n = 7; CIE n = 8; WD n = 7; * = $p < 0.05$; ~50 kD, 10 μg protein/lane). Increased phosphorylation at Thr286 residues increases kinase activity, in addition to increasing autonomous activity. B) Increased inhibitory Thr305/306 phosphorylation during WD (CON n = 9; CIE n = 8; WD n = 7; * = $p < 0.05$; ~50 kD, 20μg protein/lane). Phosphorylation at Thr305/306 only occurs following Thr286 phosphorylation and is inhibitory for CaMKII function. This indicates CaMKII activity is down regulated during WD. C) No change in total CaMKII protein expression across treatments (n = 16 in all conditions; ~50 kD; 20 μg/lane). Indicates increases in phosphorylation are not due to increased amount of protein available for phosphorylation, and is related to kinase activity.

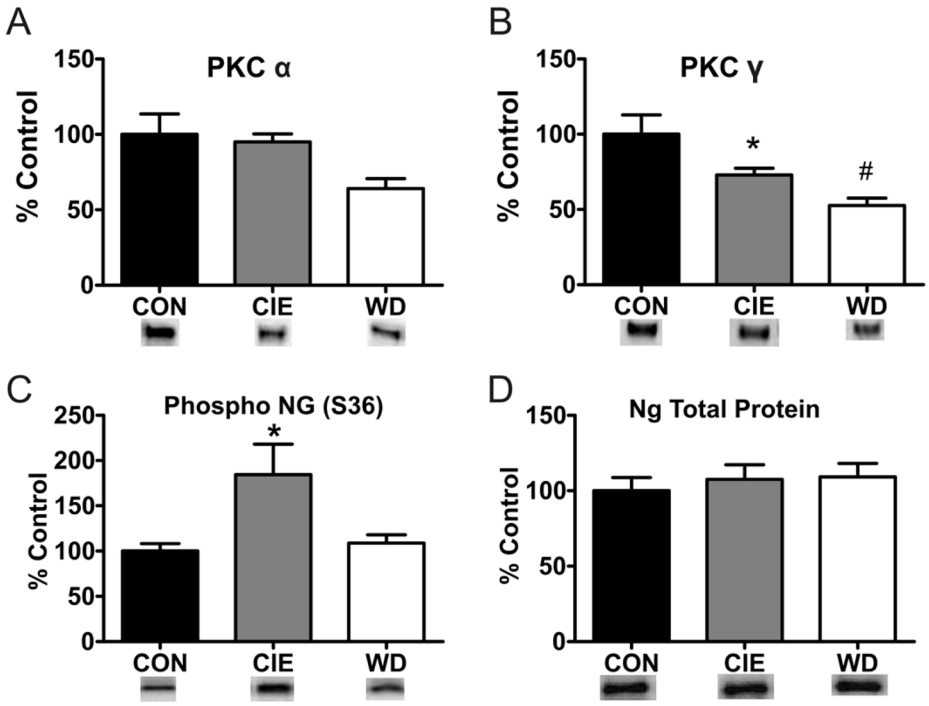

Figure 6. Dynamic treatment dependent regulation of isoform specific PKC activity and protein expression

A) Main effect for treatment dependent decrease in PKCα protein expression (n = 4 in all conditions; ~82 kD, 10μg protein/lane). B) Treatment dependent decreases of PKCγ protein expression during both CIE and WD (n = 4 in all conditions, * = $p < 0.05$, # = $p < 0.01$; ~78 kD, 10 μg protein/lane). C) Increased Ng Ser36 phosphorylation during CIE (CON, n = 8; CIE, n = 9; WD, n = 7; * = $p < 0.05$; ~7 kD, 10 μg protein/lane), with no change in total Ng protein (~7 kD; 10 μg protein/lane). D) (CON, n = 8; CIE, n = 9; WD, n = 9). Ng Ser36 phosphorylation is PKC dependent, and indicates that despite decreased PKC protein expression during CIE/WD, the activity of PKC is increased during CIE. Both PKC protein and activity are down regulated during WD.

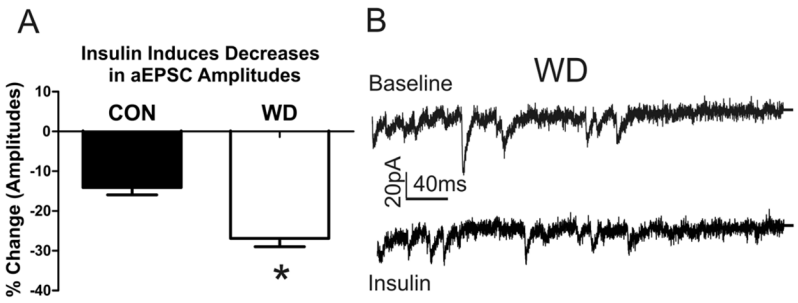

Figure 7. Insulin application decreases aEPSC amplitudes

A) Data indicates the % decrease of aEPSC amplitudes across both CON and WD treatment groups. Slice application of Insulin significantly decreased CON amplitudes and to a greater extent WD amplitudes (% Baseline, Con, −14.09±1.863%; WD, −26.89±2.103%; Unpaired t-test $t=4.555$ $df = 10$ $p < 0.01$). B) Representative traces showing insulin reduction in aEPSC during WD. Top trace represents baseline responding, while the bottom trace represents responding following insulin (1.0μM) application. Overall, these data demonstrate that regulation of AMPAR is feasible in spite of down regulated kinase activity (see Fig. 5, 6).